Comparison of the TIM and TOM Channel Activities of the Mitochondrial Protein Import Complexes

Concepción Muro,*† Serguei M. Grigoriev,† Dawn Pietkiewicz,† Kathleen W. Kinnally,† and María Luisa Campo*

*Departamento de Bioquímica y Biología Molecular y Genética, Facultad de Veterinaria, Universidad de Extremadura, 10071 Cáceres, Spain; and †Division of Basic Sciences, New York University College of Dentistry, New York, New York 10010

ABSTRACT   Water-filled channels are central to the process of translocating proteins since they provide aqueous pathways through the hydrophobic environment of membranes. The Tom and Tim complexes translocate precursors across the mitochondrial outer and inner membranes, respectively, and contain channels referred to as TOM and TIM (previously called PSC and MCC). In this study, little differences were revealed from a direct comparison of the single channel properties of the TOM and TIM channels of yeast mitochondria. As they perform similar functions in translocating proteins across membranes, it is not surprising that both channels are high conductance, voltage-dependent channels that are slightly cation selective. Reconstituted TIM and TOM channel activities are not modified by deletion of the outer membrane channel VDAC, but are similarly affected by signal sequence peptides.

INTRODUCTION

The vast majority of mitochondrial proteins are encoded in the nucleus, synthesized in the cytoplasm, and selectively imported into the organelles. Since mitochondria have two membranes, precursors targeted to the matrix must cross both barriers, presumably through proteinaceous channels (Blobel and Dobberstein, 1975; Schatz and Dobberstein, 1996). Several membrane proteins participate in this process of translocation, either through recognition of the precursors or their selective passage (Bauer et al., 2000; Jensen and Johnson, 2001; Neupert, 1997; Pfanner and Geissler, 2001; Pfanner and Truscott, 2002). Components of the import apparatus of the inner membrane, or Tim complex, in yeast mitochondria include Tim17p, Tim23p, Tim44p, and mt-Hsp70p (Ryan and Jensen, 1995). The import apparatus of the outer membrane, or Tom complex, is composed of several proteins including Tom40p, Tom70p, Tom22p, and Tom20p, as well as the small components Tom5p, Tom6p, and Tom7p (reviewed in Pfanner and Geissler, 2001; Bauer et al., 2000; Ryan and Jensen, 1995; Schatz and Dobberstein, 1996; Neupert, 1997). Whereas the import machinery of the inner and outer membranes can operate independently, current models favor their transient linkage at sites of close contact between the two membranes (Schulke et al., 1997,

1999). Recently, Tim23p has been implicated in the tethering of the Tim complex to the outer membrane (Donzeau et al., 2000).

The targeting region of a precursor protein is usually located at the amino-terminus and folds as a cationic amphiphilic α-helix (Schatz, 1993; Schatz and Dobberstein, 1996). Receptors in both complexes recognize the targeting regions and facilitate selective passage of the precursor proteins through water-filled channels. The import complexes of both membranes contain channels that provide the actual pathway for translocation of precursors across the hydrophobic region of the membranes.

Two channel activities that purportedly function in the import of proteins into mitochondria are identifiable in the mitochondrial inner and outer membranes using electrophysiological techniques (Juin et al., 1997; Künkele et al., 1998a,b; Lohret et al., 1997). The MCC is detected using patch-clamp techniques in both mammalian (Kinnally et al., 1992, 1993, 1996, 2000) and yeast mitoplasts (mitochondria treated to expose the inner membrane), as well as proteoliposomes containing purified inner membranes (Lohret and Kinnally 1995a). The activity of the PSC is associated with the outer membrane and is typically detected using the tip-dip or planar bilayer methods (Juin et al., 1997; Künkele et al., 1998a). Both MCC and PSC have large conductances suggesting their pores are of sufficient size to allow the passage of unfolded polypeptides. The activities of both MCC and PSC are specifically altered by signal peptides, synthetic peptides whose sequences mimic targeting regions of mitochondrial precursors (Juin et al., 1997; Kushnareva et al., 1999; Lohret et al., 1997; Lohret and Kinnally 1995b; Thieffry et al., 1992).

MCC and PSC are now designated the TIM and TOM channel activities, respectively. Both channels are linked to the Tim and Tom complexes by many experimental findings that are reviewed in Kinnally et al. (2000). Importantly, Lohret et al. (1997) found antibodies against Tim23p (that inhibit protein import) blocked the conductance through the

---

TIM channel and a point mutation in Tim23p modified the TIM but not TOM channel activity (Lohret et al., 1997). Immunoprecipitation of extracts with antibodies against Tom40p correlated with loss of TOM channel activity in bilayer experiments (Juin et al., 1997), and these antibodies modified the conductance of the TOM channel (Juin et al., 1997; Künkele et al., 1998a). Significantly, channel activity similar to that of TOM is detected in planar bilayers upon incorporation of purified Tom complex (Juin et al., 1997; Künkele et al., 1998a,b) and of bacterially expressed Tom40p, the general insertion pore of the Tom complex (Hill et al., 1998).

In this study, a direct comparison of the single-channel properties of the TOM and TIM channels was carried out. Patch-clamp techniques were applied to the TIM and TOM channels of wild-type yeast, a strain carrying a point mutation in Tim23p, and strains lacking VDAC.

EXPERIMENTAL PROCEDURES

Isolation of mitochondria and preparation of proteoliposomes

Most procedures were previously reported (Lohret et al., 1997) and are summarized here. Mitochondria were isolated from yeast grown in lactose media and harvested in log phase. A strain of yeast (M22-2-1) in which both isomers of VDAC had been deleted (Blachly-Dyson et al., 1997) was used, unless otherwise stated. Homogenization buffer was 0.6 M sorbitol, 10 mM Tris, 1 mM EDTA, 0.2% BSA, and 1 mM PMSF (pH 7.4) containing protease inhibitor cocktail (Sigma, P 8215). Mitoplasts were prepared from isolated mitochondria by the French press method (Decker and Greenawalt, 1977) and the outer membranes were harvested. The inner membranes were further purified according to Mannella (1982). The purity of the membrane fractions was routinely assayed, and cross-contamination was typically less than 5% for each membrane. Inner and outer membranes were separately reconstituted into giant proteoliposomes by dehydration-rehydration as previously described (Lohret et al., 1996, 1997; Lohret and Kinnally, 1995a,b) using soybean L-α-phosphatidylcholine Sigma Type IV-S. In some experiments, strain M22-2 (Blachly-Dyson et al., 1990), which was disrupted for the first isomer of VDAC, and its corresponding wild-type strain, M3, were used as the source of outer membranes (Fig. 1 A). In other experiments, the *tim23.1* strain, which carries a point mutation in Tim23p, was used as indicated (Lohret et al., 1997).

Patch-clamping techniques

All patch-clamp experiments were carried out on reconstituted TIM and TOM of proteoliposomes containing mitochondrial inner and outer membranes, respectively. Procedures and analysis used were as previously described (Lohret et al., 1997; Pavlov et al., 2001). Briefly, membrane patches were excised from giant proteoliposomes after formation of a giga seal using microelectrodes with ~0.4 μm diameter tips and resistances of 10–20 MΩ (program courtesy of A.K. Dean, Sutter Instrument, Novato, CA). Unless otherwise stated, the solution in the microelectrodes and bath was 150 mM KCl, 5 mM HEPES, pH 7.4, and the experiments were carried out at room temperature (~23°C). Peptides were introduced and removed by perfusion of the bath (0.5 mL volume) with 3–5 mL of media or included in the microelectrode filling solution. Voltage clamp was established with the inside-out excised configuration of the patch-clamp technique (Hamill et al., 1981) using a Dagan 3900 patch-clamp amplifier in the inside-out mode. Voltages across patches excised from proteoliposomes were reported as bath
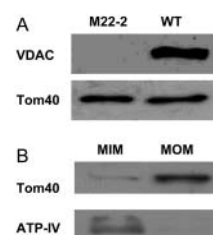

FIGURE 1 Purity of the mitochondrial inner and outer membrane preparations is high from VDACless yeast. (*A*) Western blot of mitochondrial outer membranes verify the M22-2 strain is VDAC deficient at comparable Tom40p levels. WT is wild-type. (*B*) Western blots using antisera against Tom40p and ATP-IV, proteins of the outer (MOM) and inner (MIM) membranes, show minimal cross-contamination of the inner and outer membrane preparations from VDACless M22-2 yeast. In strains that are not VDAC deficient, VDAC antisera was used in lieu of Tom40p to determine purity (e.g., as done in Fig. 8).

potentials. Channel open probability, P_O, was calculated as the fraction of the total time the channel spent in the fully open state from total amplitude histograms generated with PAT program (Strathclyde Electrophysiological Software, courtesy of J. Dempster, University of Strathclyde, Glasgow, Scotland). Unless otherwise specified, filtration was at 2 kHz with 5 kHz sampling for open probability determinations and in currents traces shown. Flicker rates were determined from current traces usually 20–40 s in duration, bandwidth limited to 2 kHz by a low pass filter, and sampled at 5 kHz. Flicker rates were the number of transition events per second from the open state to lower conductance states with a 50% threshold of the predominant event (or ~250 pS). Typically, only single-channel patches were used for the analysis of flicker blockade. Current-voltage curves are computer-generated through Clampex (Version 8.1.0.12, Axon Instruments, Union City, CA) at 5000 samples/250 s episode, from –75 to +75 mV. Simulations were generated by Electrophysiology Data Recorder V-2.2.3. software (J. Dempster, University of Strathclyde) by providing transition amplitude, τ_{open}, τ_{closed} with five openings per burst for each data set. The observed simulated distributions were identical to those predicted by fitting the open probability with a binomial distribution. That is, the distribution of time spent in each of the three states (two open ($P_{O1O2} = Po^2$), one open and one closed ($P_{O1C2 \text{ or } C1O2} = 2Po(1 - Po)$), and two closed ($P_{C1C2} = (1 - Po)^2$) was fit to the enclosed binomial equations where Po is the open probability of a single independent channel. Kinetic analysis was typically done at 5 kHz filtration and 10 kHz sampling for fast time constants. Permeability ratios were calculated from the reversal potential in the presence of a 150:30 mM KCl gradient as previously described (Lohret et al., 1997).

The following equation was used to estimate the pore size from the conductance: $R_{pore} = \rho(l/\Pi a^2)$, where R_{pore} is the resistivity of the pore, and ρ is the resistivity of the solution (80 Ω ohms-cm), l is pore length, and a is pore radius (Hille, 1992). The calculations are made from the conductance measurements assuming a pore length of 7 nm for both TIM and TOM, as this is the average thickness of a protein containing membrane. Access resistance was not included in this calculation, as this would require additional assumptions that would change the estimated pore dimensions, but would not reveal comparative differences between TIM and TOM. Interestingly, these assumptions led to a pore diameter estimate for TOM that closely corresponds to that found in single particle analysis (Künkele et al., 1998a). Unless otherwise specified, n = number of independent patches.

Peptides

Peptides shown in Table 2 were prepared by the New York State Department of Health Wadsworth Center Peptide Synthesis Core Facility (Albany, NY)

using an Applied Biosystems 431A automated peptide synthesizer as previously described (Lohret et al., 1997). Peptides were subjected to mass spectroscopy to determine impurities and proper composition, and were typically >90% pure.

Immune blotting

Samples in 10 mM Tris were diluted 1:2 into Laemmli sample buffer (0.5 mM Tris, 10% Glycerol, 10% SDS, 5% β-mercaptoethanol, 0.5% Coomassie G-250). Samples for Western blots were heated at 95°C for 5 min before electrophoresis. Mitochondrial proteins were separated by SDS-PAGE (Laemmli, 1970) and transferred to nitrocellulose or polyvinylidene difluoride membranes (Towbin et al., 1979). Filters were decorated with antibodies and visualized by chemiluminescence with ECL (Amersham, Buckinghamshire, UK).

RESULTS

The inner and outer membranes of mitochondria contain Tim and Tom complexes, respectively, that are responsible for protein import. The channel activities associated with these complexes were characterized and compared after separate reconstitution into proteoliposomes of mitochondrial inner and outer membranes from wild-type, VDACless, and Tim23p mutant yeast strains.

The purity of the membrane fractions was routinely assessed using a variety of techniques. Immunoblotting showed that, for the most part, the outer membrane channel protein, VDAC, was found only in the outer membrane preparations, and that the inner membrane protein ATP-IV was found only in the inner membrane preparation. Antiserum against the outer membrane protein Tom40p was used in lieu of VDAC in VDAC-deficient strains (see Fig. 1). Quantitative analysis of typical blots with Scion Imaging (Frederick, MD) software indicates less than 5% cross-contamination between membranes. Furthermore, VDAC channel activity was routinely observed in proteoliposomes containing outer membranes from wild-type yeast, but was very rarely detected in inner membrane preparations (<1/300 independent patches) (Lohret and Kinnally, 1995a). Finally, as discussed later, a point mutation in Tim23p modified the TIM, but not the TOM, channel activity.

Single-channel characterizations of TOM and TIM

Patch-clamp techniques were used to examine the single-channel properties of the TIM and TOM channels of the mitochondrial inner and outer membranes, respectively. High-resistance seals were formed on proteoliposomes containing either purified inner or outer membranes using microelectrodes, and the current flowing through single open channels was measured at various voltages. As shown by the current traces and the current voltage plots of Fig. 2, the conductance of the open states of the TIM and TOM channels are the same, 1000 pS. Furthermore, both channels have a major half-open state of 500 pS.
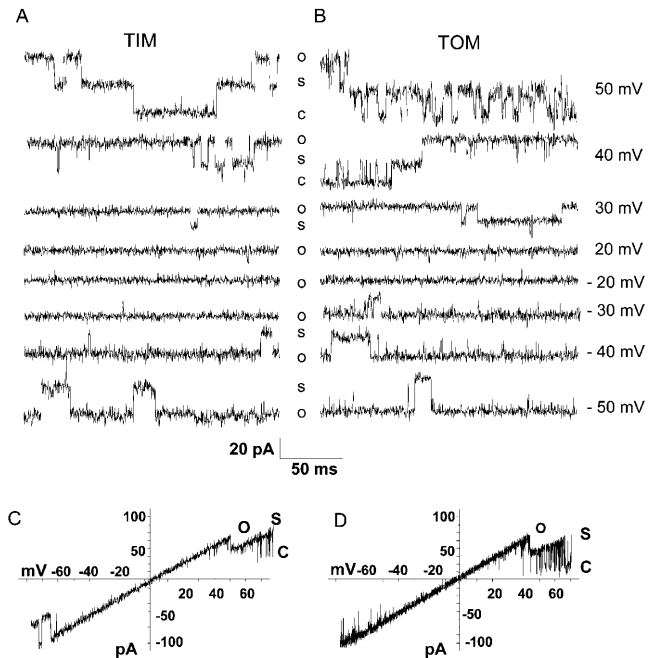

FIGURE 2 Single-channel properties of TIM and TOM channels are similar. Typical single channel current traces of TIM (*A*) and TOM (*B*) channels are shown at various voltages with 2 kHz filtration in symmetrical 150 mM KCl 5 mM HEPES, pH 7.4. Typical current-voltage relationship of single TIM (*C*) and TOM (*D*) channels reveal similar conductance levels and voltage dependence. Voltage ramps are computer generated through Clampex (Version 8.1.0.12, Axon Instruments) at 5000 samples/250 s episode, from −75 to +75 mV. O, S, and C correspond to the open (1000 pS), half-open substate (500 pS), and closed conductance levels.

TIM and TOM channels have the same function and share many single channel characteristics (see Table 1). Both channels are voltage dependent and occupy lower conductance levels at positive potentials as shown in the current traces and open probability (P_o) versus voltage plots of Figs. 2 and 3. The parameters associated with voltage dependence are indistinguishable for both channels, e.g., the gating charge and V_0 as shown in Fig. 3, *C* and *D*. Remarkably, the mean open, substate, and closed times, as well as the burst lengths, are indistinguishable as shown in Table 1. In agreement with earlier studies of TIM channels (Lohret and Kinnally, 1995a), further kinetic analysis for TIM and TOM channels showed the open, substate, and closed-time distributions could usually be best fit with one to three exponentials, supporting the existence of multiple kinetic states. As shown in Fig. 4, the dwell-time constants (which can reflect different kinetic states) are also similar for the TIM and TOM channels at different voltages. Finally, both channels are slightly cation selective with permeability ratios for P_K/P_{Cl} of ~5. This selectivity may be related to recognition of cationic presequences.

Single-particle analysis of isolated TOM complexes suggests the TOM channel has a double, and perhaps a triple, barrel structure with a pore size of ~2 nm (Künkele et al.,

TABLE 1 Electrophysiological comparison of TIM and TOM channel activities

	TIM channel		TOM channel	
Peak conductance (pS)	1160 ± 140		1060 ± 170	
Predominant transition (pS)	490 ± 43		496 ± 63	
Gating charge	-4.2 ± 0.7		-4.5 ± 1.1	
V_o (mV)	50 ± 10		50 ± 3	
Permeability of K^+/Cl^-	5.0 ± 0.3		4.7 ± 0.3	
Multiple kinetic states	>3		>3	
	+20 mV	−20 mV	+20 mV	−20 mV
Mean open time (ms)*	10.6 ± 4.3 ($n = 13$)	13.9 ± 4.7 ($n = 11$)	14.5 ± 1.4 ($n = 5$)	13.4 ± 5.5 ($n = 7$)
Mean substate time (ms)*	0.5 ± 0.2 ($n = 11$)	0.4 ± 0.1 ($n = 10$)	1.0 ± 0.5 ($n = 9$)	0.5 ± 0.4 ($n = 7$)

*Data pooled from at least four patches (n indicates independent patches) analyzed at 2 kHz filtration and 5 kHz sampling rate.

1998a; Model et al., 2002). However, little is known about the structure of the protein translocating channels of the Tim complex beyond the molecular components. Considering the similarities in function, a similar structure for the TIM and TOM channels is expected. It is interesting to note that the total amplitude histograms of Fig. 5, *B* and *D*, show that the distribution for both the TIM and TOM channels is not always binomial, as would be expected if a double-barrel pore represented two independent 500 pS channels. The amplitude histograms for both channels fit a Gaussian or binomial distribution when the open probability is high (Fig. 5, *A* and *C*), as binomial and Gaussian distributions converge when sampling is high. However, distributions that were simulated to fit the conductance level for two open and independent 500 pS channels (O) poorly fit the predicted distributions for the two closed (C) or one open/one closed (S) amplitude histograms in many experiments (Fig. 5, *B* and

D). These data suggest that the gating of putative double-barrel pores is cooperative. However, the deviation of the occupancies from predicted binomial distributions for the three states for TIM and TOM is not identical, and further studies are under way. Alternatively, the pore size of both TIM and TOM channels is significantly larger and the substate corresponds to a reduction in the pore diameter similar to the half-open state of VDAC. Experiments are under way to distinguish between these possibilities. Note that rough conductance calculations (Hille, 1992) suggest
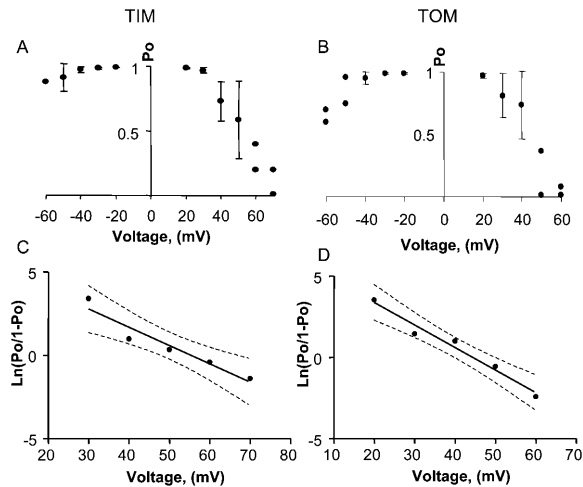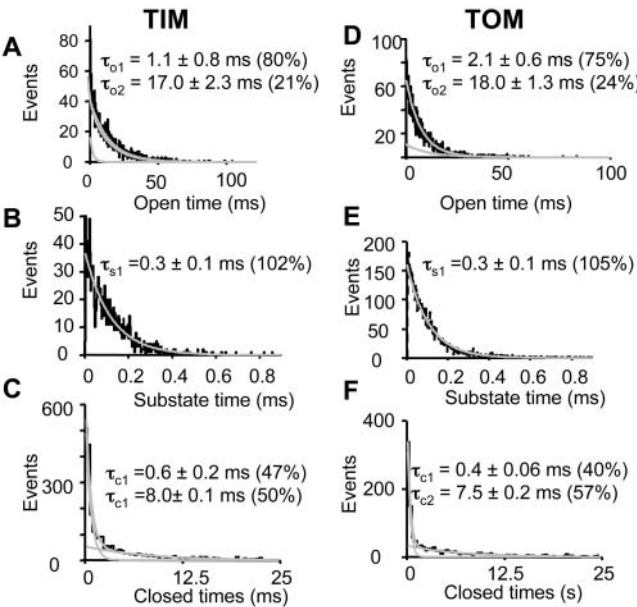

FIGURE 4 Dwell-time distributions for TIM and TOM channels. Dwell-time distributions were fit to 5000–6000 events at voltages favoring the occupation of the state examined for a typical single channel activity. Open dwell-time distributions recorded at +20 mV for typical single TIM (*A*) and TOM (*D*) channels are fit with the sum of two exponentials with 2 kHz filtration and 5 kHz sampling rate. Substate time distributions are fit with a single exponential function for the TIM channel (*B*) at +40 mV and the TOM channel at +50 mV (*E*) at 5 kHz filtration and 10 kHz sampling rate. Closed-time distributions are fit with two exponential functions for the TIM (*C*) and TOM channels at +60 mV (*F*). Fits are shown in gray and data is black. Dwell-time constants (τ) are as indicated in each plot with % contribution in parenthesis.

FIGURE 3 TIM and TOM channels are voltage dependent. The open probability (*Po*) of TIM (*A*) and TOM (*B*) channels were determined for recordings of 30-s duration at various voltages from total amplitude histograms (not shown). Gating charge is proportional to the slope of $\text{Ln}(Po/(1-Po))$ versus voltage plots and show that the gating charge of TIM (*C*) and TOM (*D*) are similar. *Po* was determined from the occupation of the 1000 pS level (O) of total amplitude histograms. Typically, points are the mean $\pm$ SD of at least eight independent patches.
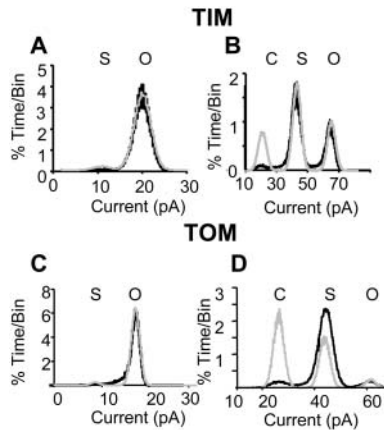
TIM

TOM

FIGURE 5   Total amplitude histograms for TIM and TOM channels can deviate from predicted binomial distributions. Total amplitude histograms are shown for TIM (A at +20 mV; B, +40 mV) and TOM (C, +20 mV; D, +30 mV) channels for experimental data (black) and data simulations (gray) fit to the probability of occupying the 1 nS level, assuming two independent channels and a binomial distribution. Simulations were generated by Electrophysiology Data Recorder V-2.2.3.software (J. Dempster, University of Strathclyde) after providing Po, transition amplitude, τ_{open}, τ_{closed} with five openings per burst for each data set (see Methods section for further details). Interval durations were binned at a resolution of 200–500 bins. Histograms are not leak subtracted.

that the estimated pore diameters of the TIM and TOM channels are sufficient to accommodate unfolded polypeptides during translocation whether they are single- or double-barrel pores, assuming a pore length of 7 nm (equivalent to the width of the native membrane) with no access resistance.

TIM and TOM channel activities are sensitive to signal peptides

The conductance of the TIM and TOM channels is regulated by synthetic signal peptides whose sequences mimic that of the targeting region found at the amino terminus of many mitochondrial precursor proteins (Lohret et al., 1997; Lohret and Kinnally, 1995b; Thieffry et al., 1992). Although the structure of the peptide SynB2 is cationic and α-helical like signal peptides, it does not support protein import into mitochondria (Allison and Schatz, 1986). Importantly, SynB2 also does not modify TIM channel activity (Lohret et al., 1997). Comparing the effect of other synthetic peptides on the TIM and TOM channel activities in wild-type yeast and a strain lacking VDAC extended these investigations. Patches of membranes were excised from the proteoliposomes containing either TIM or TOM channel activity. The conductance across each membrane was then determined in the presence and absence of signal peptides.

The addition of a peptide based on the first 13 amino acids of cytochrome oxidase subunit IV presequence (yCOX-IV$_{1-13}$) of Saccharomyces cerevisiae modified the channel activities of both the TIM and TOM channels. Transitions to the major subconductance level of 500 pS can be

visualized as downward deflections in the current traces of Fig. 6 and were relatively infrequent in the absence of peptide or in the presence of SynB2. However, current traces reveal large amplitude, rapid flickering between the open (1000 pS), subconductance (500 pS), and closed states in the presence of yCOX-IV$_{1-13}$ for both channels. There was a four- to eightfold increase in the number of transition events in the presence of yCOX-IV$_{1-13}$ compared to the absence (control) and the presence of SynB2 as shown in the histograms of Fig. 6 C for both the TIM and TOM channel activities. The effects of two signal and control peptides are summarized in Table 2. Interestingly, the dose dependence for the effect, as well as the maximal flicker rate induced, were the same for the TIM and TOM channels as shown in Fig. 6 D. The μM concentrations of the signal peptides needed to induce these effects on the two channels (Lohret et al., 1997; Lohret and Kinnally, 1995b) were similar to those known to competitively inhibit protein import (Allison and Schatz, 1986; Glaser and Cumsky 1990).

Peptide sensitivity is a voltage-dependent phenomenon in that rapid flickering and decreased open probability of the TIM and TOM channels is observed when the electrochemical gradient favors movement of the signal peptides across the membrane as shown in the voltage ramps and Po-voltage plots of Fig. 7. The occupation of the closed state (C) and substate (S) typically is seen at lower positive potentials in the presence of peptide in the bath (voltage ramps of Fig. 7, C, D, E, and F) than in its absence (Fig. 7, A and B). There is no effect at negative potentials shown in either the voltage ramps (Fig. 7, A–F) or open probability plots (Fig. 7, G and H). This shift to occupation of the substate is also seen in the amplitude histograms of Fig. 7, I and J. Furthermore, these cationic peptides are effective when placed in either the bath at positive potentials or the microelectrode at negative potentials (compare flicker rates of Fig. 6 C (peptide in bath) with Table 2 (peptide in microelectrode)). These results are consistent with an "electrophoresis" of the peptide across the membrane. As shown in Table 2 and Fig. 6 D, yCOX-IV$_{1-13}$ and yCOX-IV$_{1-22}$ modified TIM and TOM channels with similar efficacy whereas SynB2 had no effect on either channel.

The peptide sensitivity of the TIM channel activity is suppressed compared to the wild-type activity by a point mutation in the protein import deficient strain tim23.1 as shown in the current traces and histograms of Fig. 8 (Lohret et al., 1997). Rapid flickering of the TOM channel is induced by signal peptide, but the TIM channel from the tim23.1 strain is relatively unaffected. This modified behavior of the TIM channel was never seen in proteoliposomes containing outer membranes, and VDAC and TOM channel activities were never observed in proteoliposomes containing inner membranes from the tim23.1 strain. The TOM channel of this strain is peptide sensitive, as it is from wild-type and VDAC-deficient yeast. The purity of the inner and outer membrane preparations from the tim23.1 strain is high as shown in
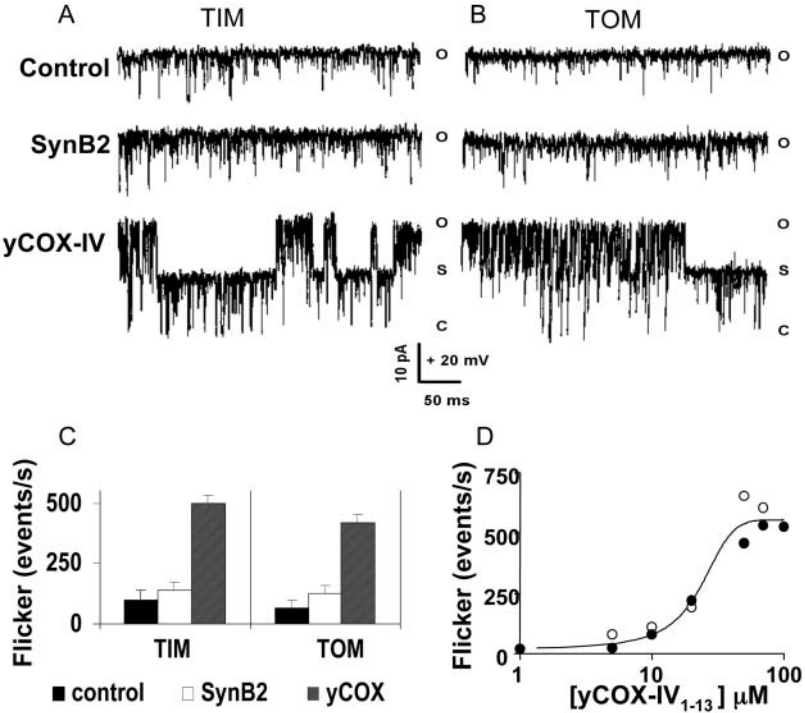
FIGURE 6 Signal peptides modulate the flicker frequency of the TIM and TOM channel activities. Typical current traces are shown at $+20$ mV for TIM (A) and TOM (B) channels in excised patches before (control, no peptide) and after sequential perfusions of the bath with 50 μM of the control peptide SynB2 and then with 50 μM of the signal peptide yCOX-IV$_{1-13}$. (C) The histograms of flicker rates (number of transition events per second) in the absence (control) and presence of SynB2 or yCOX-IV$_{1-13}$ are similar for the TIM and TOM channels. (D) The dose dependence of the flicker rate on the concentration of peptide yCOX-IV$_{1-13}$ is shown for TIM (o) and TOM ($\bullet$) channels. Other conditions are as in Fig. 2.

the Western blots of Fig. 8 C. Undetectable levels of the outer membrane protein VDAC are in the inner membrane preparation whereas undetectable levels of the inner membrane protein ATP-IV are in the outer membrane preparation.

DISCUSSION

Blobel and Dobberstein (1975) postulated that proteins were translocated across membranes through water-filled channels. Patch-clamp techniques provide unique and novel methods for examining the functional characteristics of these aqueous pores and enable dissection of the function of their components. This study represents the first direct comparison of channel modulation by signal peptides of the Tom and Tim complexes, the protein import machinery of mitochondrial outer and inner membranes, respectively. Both complexes contain pores and receptors that recognize and facilitate the translocation of the precursors.

Signal peptides modulate the activity of the TIM and TOM channels

The protein import apparatus interacts with targeting regions of precursors (Blobel and Dobberstein, 1975). Therefore, it is not surprising that the activities of the TIM and TOM channels were modulated by signal peptides as shown in Table 2. Similar concentrations of these peptides induced approximately the same flicker rates in the two different channels (Fig. 6 D and Table 2). Interestingly, protein import was competitively inhibited by equivalent concentrations of signal peptides (Allison and Schatz, 1986; Glaser and Cumsky, 1990).

At this time, the nature of the flicker events is not well defined. The duration of the events is typically 400–700 μs, suggesting an interaction of the signal peptides with the channels. Although it is proposed that these events reflect transient occlusion of the pore of the channel during translocation of the peptides, such translocation events are expected to be significantly faster, tens of nanoseconds rather

TABLE 2   The effects of peptides on flickering of TIM and TOM channels

Peptide	Sequence	Source	Net charge	Signal peptide	μM pipette	TIM events/s	TOM events/s
yCOX-IV$_{1-13}$	[1]MLSLRQSIRFFKY$_{13}$	Yeast	$+3$	yes*	50	275 ± 30	270 ± 35
yCOX-IV$_{1-22}$	[1]MLSLRQSIRFFKPATRTLCSSR$_{22}$	Yeast	$+5$	yes*	30	280 ± 25	275 ± 25
SynB2	[1]MLSRQQSQRQSRQQSQRQSR$_{20}$	Synthetic	$+5$	no[†]	50	60 ± 15	66 ± 13

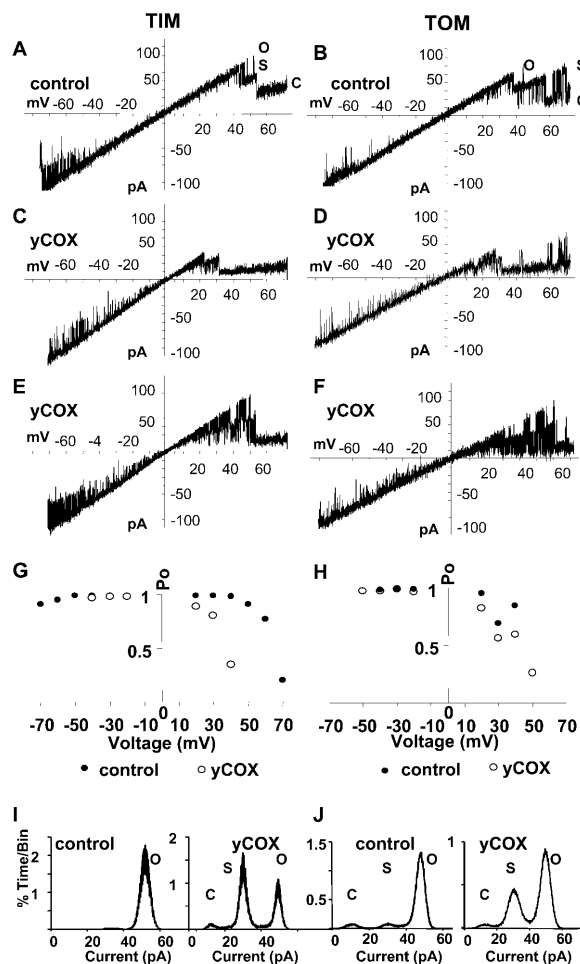*Glaser and Cumsky (1990).
[†]Allison and Schatz (1986).

FIGURE 7 Voltage dependence of the open probability of the TIM and TOM channels is modified by signal peptides. Current voltage curves are shown for a single TIM (A, C, E) and TOM (B, D, F) channel in the absence and presence of 50 μM yCOX-IV$_{1-13}$ in the bath as indicated. Note that the channels show a decrease in open probability (C, D) as well as rapid flickering (E, F) in the presence of signal peptide at positive but not negative potentials. Open probability voltage curves are shown for TIM (G) and TOM (H) in the absence ($\bullet$) and presence ($\circ$) of yCOX-IV$_{1-13}$. Total amplitude histograms are shown for TIM (I) and TOM (J) channels in the absence (control) and presence of yCOX-IV$_{1-13}$ peptide at +40 mV.

FIGURE 8 Mutation in Tim23p distinguishes TIM from TOM channel activity. (A) Current traces of TIM and TOM channels are shown in the presence and absence of 50 μM yCOX-IV$_{1-13}$ and illustrate the decrease in peptide sensitivity of TIM but not TOM in the *tim23.1* strain. (B) Histograms show the peptide sensitivity as indicated by flicker rate of the TIM channel is reduced; the TOM channel of this strain is identical to that of wild-type yeast. (C) Western blots show the cross-contamination of the preparations is low when probing with VDAC antisera for the outer membrane and ATP-IV antisera for the inner membrane.

than hundreds of microseconds, for polymers of this length if there is no interaction with the pore (Kasianowicz et al., 1996). Similarly, correlations have been made between the duration of blockade and polymer length in studies of RNA and DNA translocation through the hemolysin channel (Akeson et al., 1999), and the type of blockade of VDAC by nucleotides (Rostovtseva and Bezrukov, 1998; Rostovtseva et al., 2002) and maltoporin by maltodextrins (Kullman et al., 2002). However, it may be important to note that fluorescently labeled yCOX-IV$_{1-13}$ and yCOX-IV$_{1-22}$ are accumulated in mitochondria in an energy-dependent manner whereas SynB2 is not sequestered (unpublished results of Grigoriev, Chopra, Dejean, and Kinnally). Hence, these events represent both unresolved interaction and translocation events.
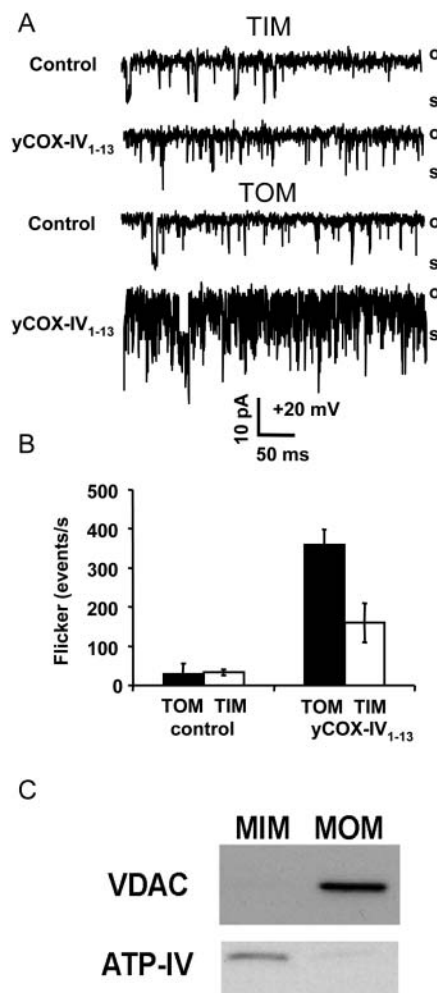
The sensitivity of the channels to signal peptide is a voltage-dependent phenomenon. The flicker rates increase with positive potentials if the peptides are located in the bath and have little effect at negative potentials. Conversely, the flicker rates increase with negative potential if the peptides are located in the microelectrodes and have little effect at positive potentials (data not shown). Intriguingly, the flicker rates induced by 50 μM peptide in the bath at +20 mV are consistently greater than the rates if peptides are in the microelectrode at −20 mV for both the TIM and TOM channels (Fig. 6 D and Table 2). These observations may be related to the voltage dependence of the channels as suggested by Kasianowicz et al. (1996) in blockade of hemolysin by single-stranded DNA molecules. Alterna-

tively, the disparity of flicker rates may be due to variations in the effective peptide concentration (possibly by chelation of the peptide by the micropipette glass). These observations may also be a reflection of different binding affinities at sites located on the two membrane faces of the channels, or differences in the structure of the two membrane faces of the channels.

The current study was, for the most part, carried out in a strain of yeast in which the two isoforms of VDAC were deleted. No effect on the regulation by signal peptides of the two activities is detected when compared to those of the wild-type strain. Furthermore, the channel activity recorded from the native inner membranes of mitochondria isolated from a yeast strain carrying a single VDAC deletion is identical to that recorded from proteoliposomes prepared with the inner membranes of mitochondria isolated from the wild-type (VDAC-containing) strain (Kinnally et al., 1996) or, as shown in this study, the double deletion mutant. These findings indicate that VDAC is not tightly linked to the normal channel activities of the two import complexes under reconstituted conditions.

The pores of the TIM and TOM channels

Although not precise, the pore diameter of a large channel can be estimated from the conductance, which is proportional to the resistance to ion flow (Hille, 1992). Since the K^+ conductances of the TIM and TOM channels are indistinguishable, these equations must generate the same size pore if the same assumptions are made for both channels. Hence, these calculations suggest the overall dimensions of the aqueous pathways of the two channels are indistinguishable. However, it is interesting that a pore diameter for both channels of ∼2.7 nm is calculated assuming a pore length of 7 nm, and no access resistance. Alternatively, the single-channel behaviors of TIM and TOM are also consistent with double-barrel pore structures. Typically, two conductance levels of 500 pS are observed with coordinated gating for both channels (Lohret et al., 1997; Lohret and Kinnally, 1995a). If this is the case, the paired conductances of ∼500 pS predict pore diameters of ∼1.9 nm for each barrel, assuming a pore length of 7 nm and no access resistance. Importantly, the inferred pore diameters of 1.9–2.7 nm (depending on the single or double pore structure) for the TIM and TOM channels should still be sufficient to allow the passage of unfolded polypeptides. Consistent with the predictions of a double-barrel pore structure based on single-channel behavior, the single-particle image analysis of purified Tom complex shows two, and possibly three, apparent ∼2 nm holes that may represent individual TOM channel pores (Künkele et al., 1998a; Model et al., 2002). Note, the failure of state occupancy to fit binomial distributions in total amplitude histograms suggests that these putative double barrels, if they exist, cooperatively gate. However, Schwartz and Matouschek (1999) estimated the pore sizes of 2.6 nm and near 2.0

nm for the TOM and TIM channels from the transport of rigid molecules and gold particles, suggesting TOM may be a large pore and TIM may be a double-barrel pore. Considering each technique has limitations, together, these findings suggest the aqueous pathways through both channels are similar but the TIM channel may have an obstruction to the flow of large molecules that is not evident in the TOM channel.

CONCLUSIONS

In this study, the single-channel activities of the Tim and Tom complexes from VDACless and wild-type mitochondria were found to be remarkably similar. The peptide sensitivity of the TIM but not the TOM channel is modified by a point mutation in Tim23p. Neither reconstituted channel activity is modified by deletion of VDAC, an outer membrane channel. The TIM and TOM channels are both high-conductance, voltage-dependent channels that are slightly cation selective. Although the proteins that constitute the channels are not the same, the TIM and TOM channels have the same function. Hence, the similarities are not so surprising. Importantly, the pores of both channels are large enough to provide passage for an α-helical or unfolded protein across a mitochondrial membrane.

REFERENCES

Akeson, M., D. Branton, J. J. Kasianowicz, E. Brandin, and D. W. Deamer. 1999. Microsecond time-scale discrimination among polycytidylic acid, polyadenylic acid, and polyuridylic acid as homopolymers or as segments within single RNA molecules. *Biophys. J.* 77:3227–3233.

Allison, D. S., and G. Schatz. 1986. Artificial mitochondrial presequences. *Proc. Natl. Acad. Sci. USA.* 83:9011–9015.

Bauer, M. F., S. Hofmann, W. Neupert, and M. Brunner. 2000. Protein translocation into mitochondria: the role of TIM complexes. *Trends Cell Biol.* 10:25–31.

Blachly-Dyson, E., S. Peng, M. Colombini, and M. Forte. 1990. Selectivity changes in site-directed mutants of the VDAC ion channel: Structural implications. *Science.* 247:1233–1236.

Blachly-Dyson, E., J. M. Song, W. J. Wolfgang, M. Colombini, and M. Forte. 1997. Multicopy suppressors of phenotypes resulting from the

absence of yeast VDAC encode a VDAC-like protein. *Mol. Cell. Biol.* 10:5727–5738.

Blobel, G., and B. Dobberstein. 1975. Transfer of proteins across membranes. I. Presence of proteolytically processed and unprocessed nascent immunoglobulin light chains on membrane-bound ribosomes of murine myeloma. *J. Cell Biol.* 67:835–851.

Decker, G. L., and J. W. Greenawalt. 1977. Ultrastructural and biochemical studies of mitoplasts and outer membranes derived from French-pressed mitochondria. *J. Ultrastr. Res.* 59:44–56.

Donzeau, M., K. Kaldi, A. Adam, S. Paschen, G. Wanner, B. Guiard, M. F. Bauer, W. Neupert, and M. Brunner. 2000. Tim23 links the inner and outer mitochondrial membranes. *Cell.* 101:401–412.

Glaser, S. M., and M. G. Cumsky. 1990. Localization of a synthetic presequence that blocks protein import into mitochondria. *J. Biol. Chem.* 265:8817–8822.

Hamill, O. P., A. Marty, E. Neher, B. Sakmann, and F. J. Sigworth. 1981. Improved patch-clamp techniques for high-resolution current recording from cells and cell-free membrane patches. *Pflügers Arch-Eur J Physiol.* 381:85–100.

Hill, K., K. Model, M. T. Ryan, K. Dietmeier, F. Martin, R. Wagner, and K. Pfanner. 1998. Tom40 forms the hydrophilic channel of the mitochondrial import pore for preproteins. *Nature.* 395:516–521.

Hille, B. 1992. Ionic Channels of Excitable Membranes, 2nd ed. Sinauer Associates, Sunderland, MA.

Jensen, R. E., and A. E. Johnson. 2001. Opening the door to mitochondrial protein import. *Nat. Struct. Biol.* 8:1008–1010.

Juin, P., M. Thieffry, J. Henry, and F. M. Vallette. 1997. Relationship between the peptide-sensitive channel and the mitochondrial outer membrane protein translocation machinery. *J. Biol. Chem.* 272:6044–6050.

Kasianowicz, J. J., E. Brandin, D. Branton, and D. W. Deamer. 1996. Characterization of individual polynucleotide molecules using a membrane channel. *Proc. Natl. Acad. Sci. USA.* 93:13770–13773.

Kinnally, K. W., Y. N. Antonenko, and D. B. Zorov. 1992. Modulation of inner mitochondrial membrane channel activity. *J. Bioenerg. Biomembr.* 24:99–110.

Kinnally, K. W., T. A. Lohret, M. L. Campo, and C. A. Mannella. 1996. Perspectives on the mitochondrial multiple conductance channel. *J. Bioenerg. Biomembr.* 28:115–123.

Kinnally, K. W., C. Muro, and M. L. Campo. 2000. MCC and PSC, the putative protein import channels of mitochondria. *J. Bioenerg. Biomembr.* 32:47–54.

Kinnally, K. W., D. B. Zorov, Y. N. Antonenko, S. H. Snyder, M. W. McEnery, and H. Tedeschi. 1993. Mitochondrial benzodiazepine receptor linked to inner membrane ion channels by nanomolar actions of ligands. *Proc. Natl. Acad. Sci. USA.* 90:1374–1378.

Kullman, L., M. Winterhalter, and S. M. Bezrukov. 2002. Transport of maltodextrins through maltoporin: a single-channel study. *Biophys. J.* 82:803–812.

Künkele, K. P., S. Heins, M. Dembowski, F. E. Nargang, R. Benz, M. Thieffry, J. Walz, R. N. Lill, S. Nussberger, and W. Neupert. 1998a. The preprotein translocation channel of the outer membrane of mitochondria. *Cell.* 93:1009–1019.

Künkele, K. P., P. Juin, C. Pompa, F. E. Nargang, J.-P. Henry, W. Neupert, R. Lill, and M. Thieffry. 1998b. The isolated complex of the translocase of the outer membrane of mitochondria. *J. Biol. Chem.* 273:31032–31039.

Kushnareva, Y. E., M. L. Campo, K. W. Kinnally, and P. M. Sokolove. 1999. Signal presequences increase mitochondrial permeability and open the multiple conductance channel. *Arch. Biochem. Biophys.* 366:107–115.

Laemmli, U. K. 1970. Cleavage of structural proteins during assembly of the head of bacteriophage T4. *Nature (Lond.).* 227:680–685.

Lohret, T. A., R. E. Jensen, and K. W. Kinnally. 1997. Tim23, a protein import component of the mitochondrial inner membrane, is required for normal activity of the multiple conductance channel, MCC. *J. Cell Biol.* 137:377–386.

Lohret, T. A., and K. W. Kinnally. 1995a. Multiple conductance channel activity of wild-type and voltage-dependent anion-selective channel (VDAC)-less yeast mitochondria. *Biophys. J.* 68:2299–2309.

Lohret, T. A., and K. W. Kinnally. 1995b. Targeting peptides transiently block a mitochondrial channel. *J. Biol. Chem.* 270:15950–15953.

Lohret, T. A., R. C. Murphy, T. Drgon, and K. W. Kinnally. 1996. Activity of the mitochondrial multiple conductance channel is independent of the adenine nucleotide translocator. *J. Biol. Chem.* 271:4846–4849.

Mannella, C. A. 1982. Structure of the outer mitochondrial membrane: ordered arrays of porelike subunits in outer membrane fractions from Neurospora crassa mitochondria. *J. Cell Biol.* 94:680–687.

Model, K., T. Prinz, T. Ruiz, M. Radermacher, T. Krimmer, W. Kuhlbrandt, N. Pfanner, and C. Meisinger. 2002. Protein translocase of the outer mitochondrial membrane: role of import receptors in the structural organization of the TOM complex. *J. Mol. Biol.* 316:657–666.

Neupert, W. 1997. Protein import into mitochondria. *Annu. Rev. Biochem.* 66:867–917.

Pavlov, E. V., M. Priault, D. Pietkiewicz, E. H. Cheng, B. Antonsson, S. Manon, S. J. Korsmeyer, C. A. Mannella, and K. W. Kinnally. 2001. A novel, high conductance channel of mitochondria linked to apoptosis in mammalian cells and Bax expression in yeast. *J. Cell Biol.* 155:725–732.

Pfanner, N., and A. Geissler. 2001. Versatility of the mitochondrial protein import machinery. *Nat. Rev. Mol. Cell Biol.* 2:339–349.

Pfanner, N., and K. N. Truscott. 2002. Powering mitochondrial protein import. *Nat. Struct. Biol.* 9:234–236.

Rostovtseva, T. K., and S. M. Bezrukov. 1998. ATP transport through a single mitochondrial channel, VDAC, studied by current fluctuation analysis. *Biophys. J.* 74:2365–2373.

Rostovtseva, T. K., A. Komarov, S. M. Bezrukov, and M. Colombini. 2002. Dynamics of nucleotides in VDAC channels: structure-specific noise generation. *Biophys. J.* 82:193–205.

Ryan, K. R., and R. E. Jensen. 1995. Protein translocation across mitochondrial membranes: what a long, strange trip it is. *Cell.* 83:517–519.

Schatz, G. 1993. The protein import machinery of mitochondria. *Protein Sci.* 2:141–146.

Schatz, G., and B. Dobberstein. 1996. Common principles of protein translocation across membranes. *Science.* 271:1519–1526.

Schulke, N., N. B. Sepuri, D. M. Gordon, S. Saxena, A. Dancis, and D. Pain. 1999. A multisubunit complex of outer and inner mitochondrial membrane protein translocases stabilized in vivo by translocation intermediates. *J. Biol. Chem.* 274:22847–22854.

Schulke, N., N. B. V. Sepuri, and D. Pain. 1997. In vivo zippering of inner and outer mitochondrial membranes by a stable translocation intermediate. *Proc. Natl. Acad. Sci. USA.* 94:7314–7319.

Schwartz, M. P., and A. Matouschek. 1999. The dimensions of the protein import channels in the outer and inner mitochondrial membranes. *Proc. Natl. Acad. Sci. USA.* 96:13086–13090.

Thieffry, M., J. Neyton, M. Pelleschi, F. Fèvre, and J.-P. Henry. 1992. Properties of the mitochondrial peptide-sensitive cationic channel studied in planar bilayers and patches of giant liposomes. *Biophys. J.* 63:333–339.

Towbin, H., T. Staehelin, and J. Gordon. 1979. Electrophoretic transfer of proteins for polyacrylamide gels to nitrocellulose sheets: procedure and some applications. *Proc. Natl. Acad. Sci. USA.* 76:4350–4354.